Hindawi
Advances in Polymer Technology
Volume 2022, Article ID 9115873, 9 pages
https://doi.org/10.1155/2022/9115873

Research Article

Well-Distributed Polysilsesquioxane-Modified Carbon Nanotubes for Thermal Conductive Insulating Silicone Rubbers

Long Han, Zhaobo Wang, Jing Hua, and Jieting Geng

Key Laboratory of Rubber-Plastics Ministry of Education/Shandong Provincial Key Laboratory of Rubber-Plastics, College of Polymer Science and Engineering, Qingdao University of Science and Technology, Qingdao 266042, China

Correspondence should be addressed to Jieting Geng; 13475862646@163.com

Received 2 May 2022; Accepted 29 July 2022; Published 27 August 2022

Academic Editor: Sagar Roy

Despite carbon nanotubes (CNTs) have garnered tremendous research interests for enhancing the electrical and thermal conductivity of polymers, it is still a considerable challenge to achieve the uniform dispersion of carbon nanotubes in polymer matrix. Herein, inspired by the mussel-inspired chemistry, we adopted the strategy of coating CNTs with polydopamine. And the polysilsesquioxane-modified CNTs (CNTs-PSQ) were obtained based on the click chemistry reaction. The FT-IR, Raman, XRD, and TGA collectively demonstrated the successful modification of PSQ on the surface of CNTs. The incorporation of PSQ could significantly improve the dispersion of CNTs in the silicon rubbers, and a strong interfacial interaction was formed between CNTs-PSQ and silicon rubber matrix, as observed from TEM images of silicon rubber/CNTs-PSQ nanocomposites. Meanwhile, compared with the nanocomposites with neat CNTs, the ones with CNTs-PSQ exhibited simultaneously improved electrical conductivity and insulating performance. This strategy proposed for the preparation of PSQ-modified CNTs provides insights toward highly insulating and thermal conducting polymers.

1. Introduction

In recent years, with the increasing integration density and power density of electronic devices, the electronic components are subjected to higher heat emissions when they are in operation. However, most of the existing materials have poor thermal conductivity, which would prevent the heat generation inside them from being released and ultimately degrade the stability and service life of electronic devices [1–3]. Therefore, how to enhance the thermal conductivity of materials without sacrificing their insulating performance has been a significant research focus for next-generation high-integration, large-area electronic devices. Gao et al. [4] designed a boron nitride-polyethersulfone/polyvinylidene fluoride (BN-PES/PVDF) composite with a neuron-like network and highly oriented structure by a facile and scalable method. This unique microstructure based on Schiff base and covalent bonds provides effective and robust phonon pathways for heat transfer. Guo et al. [5] fabricated a PA6/BN composite via in situ polymerization and melt blending with polyamide-6 (PA6). The masterbatch-based melt lending strategy is conducive to form effective thermal pathways for phonon transmission and decrease the interfacial thermal resistance of the PA6 matrix. Li et al. [6] prepared a highly thermal-conductive material with reasonable bonding force on a Cu substrate by sequential immersion deposition in a dopamine solution and an aqueous graphene oxide (GO) suspension.

Recently, CNTs have attracted extensive attention from the academy and industry due to their distinct advantages such as high mechanical robustness [7–9], high electrical conductivity [10, 11], high thermal conductivity [12, 13], and good compatibility with elastomeric polymers [14]. It is universally acknowledged that the good dispersion of CNTs in the polymer matrix was the prerequisite to ensure the improved mechanical properties of the nanocomposites. Therefore, the blending process of CNTs in the polymer matrix is extremely significant. However, the uniform dispersion of CNT particles in polymer matrix remains a considerable challenge, accounting for the fact that the high aspect ratio of nanotubes and large van der Waals force among tubes easily accelerate the entanglement of CNTs

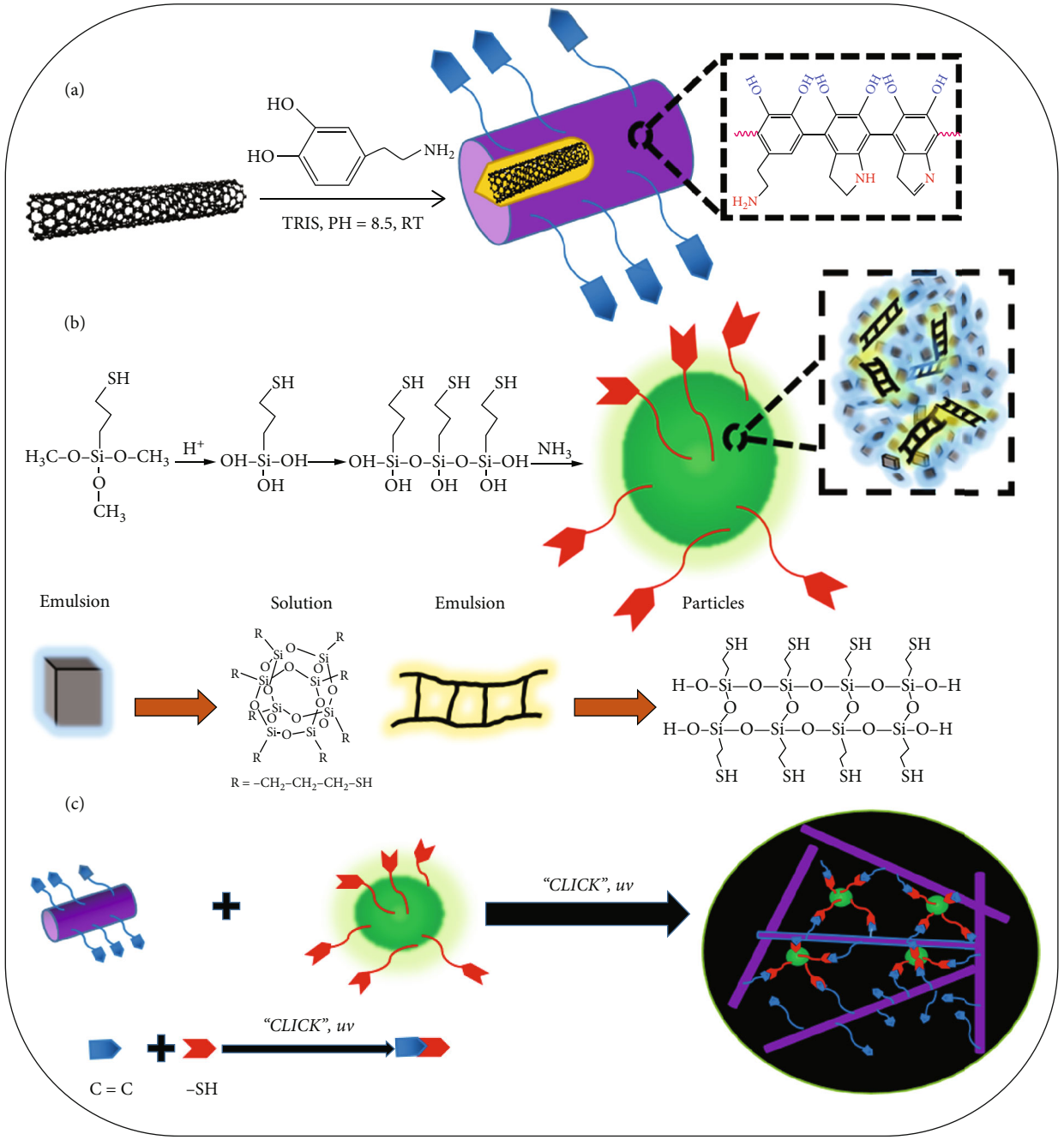

Figure 1: Schematic representation of the synthetic route from CNTs to CNTs-PDA and CNTs-PSQ.

[15, 16]. Over the past few decades, tremendous efforts have been devoted to surface modification of CNTs via the covalent and noncovalent strategies [17–19]. But unfortunately, the strategies show inevitable disadvantages. For example, the covalent strategy often involves hazardous chemical agents, harsh reaction conditions, and complicated fabrication procedures, while the noncovalent strategy is strongly dependent on the self-assembly of CNTs and amphiphilic materials, which largely restricts the application of CNTs in the functional polymers [20, 21]. Thus, it is an urgent task to employ a simple and effective approach to uniformly disperse CNT particles in the polymer matrix.

Marine mussels have a superior ability for adhering to various surfaces [22–25]. The strong adhesive force between the mussels and surface of materials is due to the existence of mussel adhesive proteins. Inspired by this, a novel surface modification strategy had been developed by Lee et al. [26] in 2007. They demonstrated that dopamine could self-polymerize under an alkaline solution and form a polydopamine (PDA) coating. The PDA coating could further react with amino or thiol functional groups through Michael's addition reaction [27]. Because of its simplicity, universality, and effectiveness, mussel-inspired chemistry has emerged as a very useful surface functionalization strategy, which has

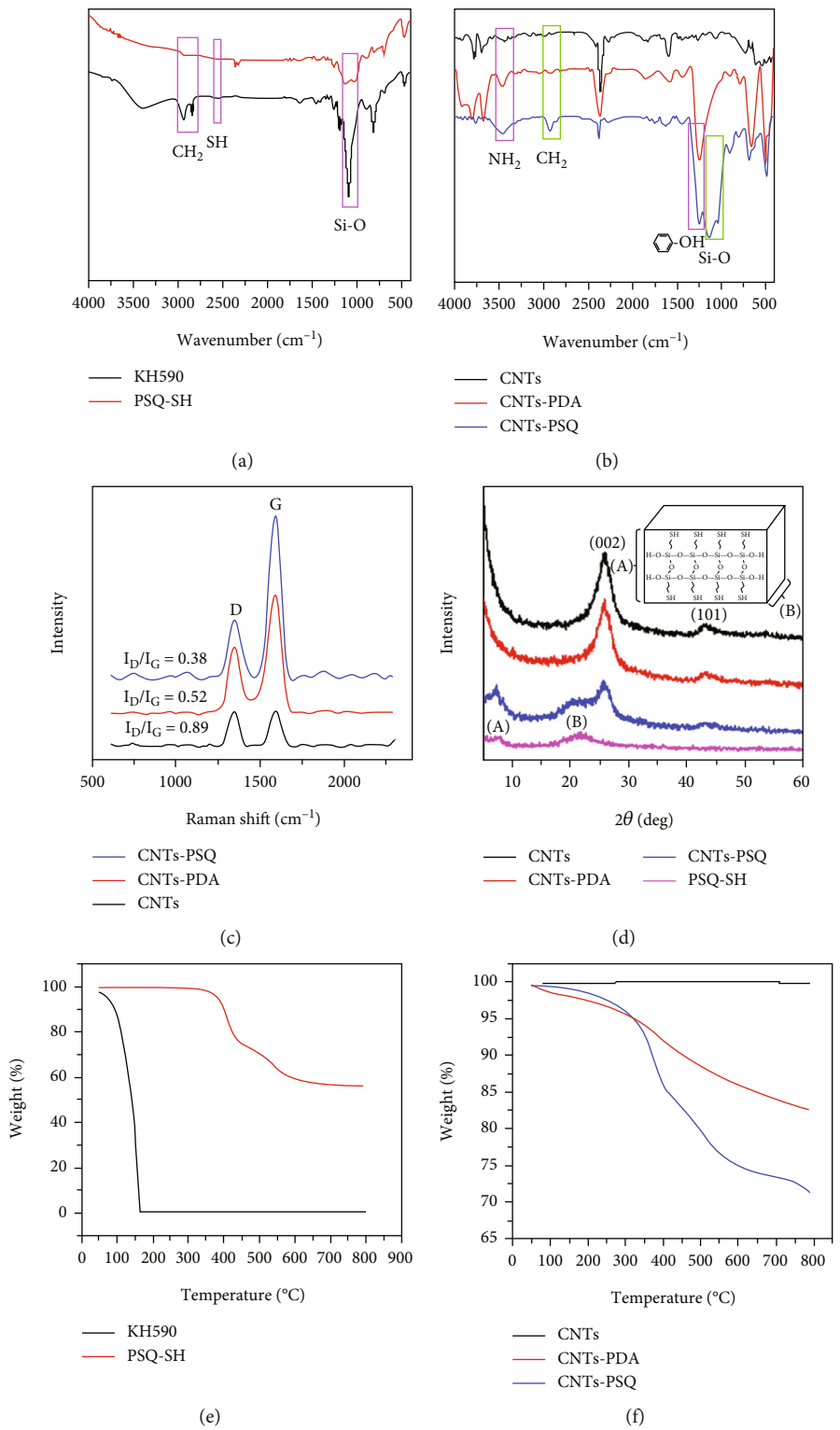

Figure 2: (a) FT-IR spectra of KH590 and PSQ-SH. (b) FT-IR spectra of pristine CNTs, CNTs-PDA, and CNTs-PSQ. (c) Raman spectra of pristine CNTs, CNTs-PDA, and CNTs-PSQ. (d) XRD spectra of PSQ-SH, pristine CNTs, CNTs-PDA, and CNTs-PSQ. (e) TGA diagrams of KH590 and PSQ-SH. (f) TGA diagrams of pristine CNTs, CNTs-PDA, and CNTs-PSQ.

been extensively explored for different applications, such as 3D centrifugal spinning [28], hydrogel [29–31], and antibacterial materials [32].

Polyhedral oligomeric silsesquioxane (PSQ), as an organic-inorganic hybrid constituent, shows a unique cage-like molecular structure and excellent physicochemical

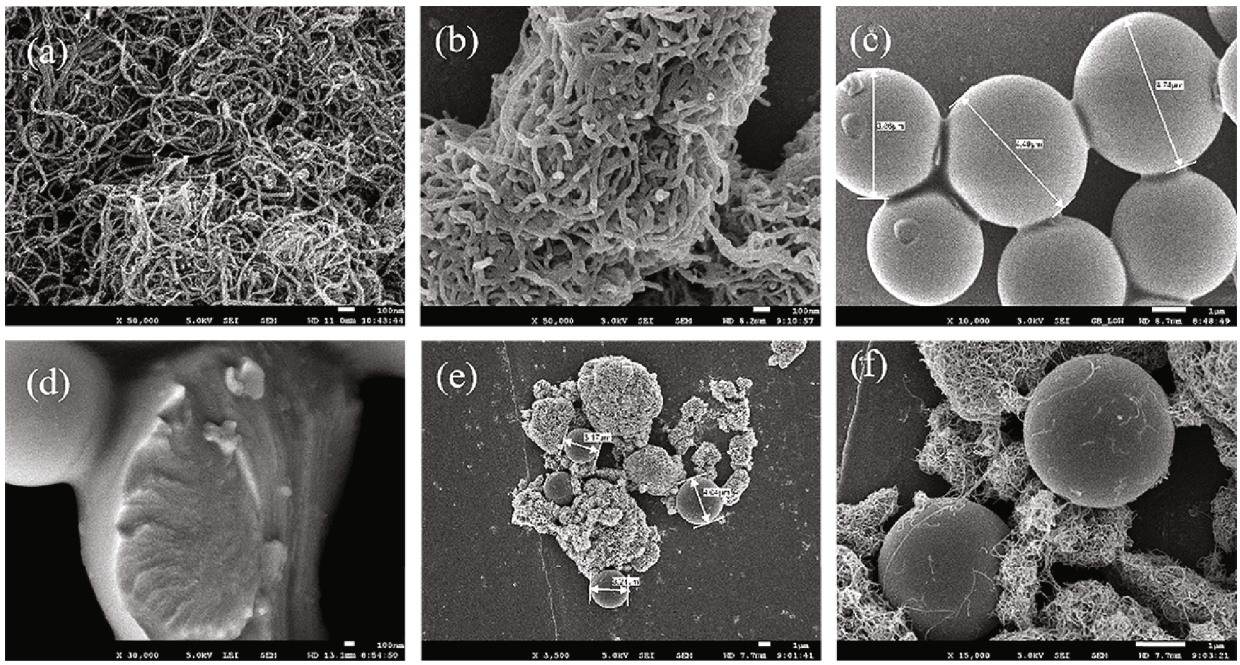

Figure 3: (a) SEM images of raw CNTs. (b) SEM images of CNTs-PDA. (c) SEM images of PSQ-SH particle. (d) SEM images of crushed PSQ-SH particle. (e, f) SEM images of CNTs-PSQ.

properties, including good thermal conductivity and insulation performance [33–35]. The inorganic inner core possesses a cage-like arrangement of silicon and oxygen atoms, and the organic groups distribute in the outer layer, which thus provide plenty of reaction sites for further functionalization.

In view of this mussel-inspired chemistry strategy, we first prepared polydopamine-coating CNTs and further obtained PSQ-modified CNTs (CNTs-PSQ) based on the click chemistry. The modification of PSQ could significantly enhance the dispersion uniformity of CNTs into the SR matrix. Surface morphology analyses indicated that a good interface between the nanofillers and the rubber matrix was formed. This rubber composite is endowed with higher thermal conductivity and insulation properties compared with its counterparts. The mussel-inspired chemistry strategy proposed herein for CNT surface functionalization is expected to be applied in high-insulation and thermal-conductive rubber materials.

2. Experimental

2.1. Materials. Multiwalled carbon nanotubes (CNTs, purity > 95 wt%, ID: 2-5 nm, length: 10-30 μm) were provided by Zhongke Times Co., Ltd. Dopamine was supplied by Sinopharm Chemical Reagent Co., Ltd. (Shanghai, China). Tris (hydroxymethyl)-methyl aminomethane (Tris, AR), HCl (38 wt % aqueous solution), ethanol (AR), and NaOH (AR) were all purchased from the Sinopharm Group. KH590 was purchased from Dow Corning Co. Tetrahydrofuran and dimethoxy-a-phenyl acetophenone (DMPA) were supplied by Shanghai Macklin Biochemical Technology Co., Ltd. Silicone rubber was purchased from Shenzhen Chuangyou Silicone Rubber Products Co., Ltd.

2.1.1. Polydopamine-Coated CNTs (CNTs-PDA). The preparation of polydopamine-coated CNTs was described as follows: 12.1 g of Tris was dissolved into 1 L of water to obtain a 0.1 mol/L Tris solution. 3.1 mL of hydrochloric acid was dissolved into 1 L of water to obtain a 0.1 mol/L hydrochloric acid solution. Subsequently, 50 mL of Tris solution (0.1 mol/L) and 14.7 mL of hydrochloric acid solution (mol/L) were mixed and diluted to 100 mL with water to prepare the Tris buffer solution with a pH value of 8.5. After that, 0.5 g CNTs were added into the Tris buffer solution through ultrasonication for 10 min, followed by the addition of 0.5 g of dopamine hydrochloride. To improve the dispersion of CNTs, the mixed solution was stirred at room temperature for 24 h and then centrifuged and oven-dried, followed by filtering with a microporous membrane and repeated washing with ethanol and deionized water. Finally, the composites were dried at 60°C for 24 h to remove the residual solvents and impurities.

2.1.2. Preparation of Sulfhydryl Polysilsesquioxane (PSQ-SH). PSQ-SH was prepared by hydrolysis and condensation of KH590, as depicted as follows: 1.6 mL of HCl solution (0.1 mol/L) was added into 80 mL of deionized water, followed by the addition of 10 mL of KH590 and continuous stirring for 18 h at room temperature. After that, 0.1 mL of triethylamine was added to the mixed solution and stirred for 30 min, followed by the centrifugal separation, filtering with microporous membrane, and repeated washing with ethanol and deionized water. Finally, the resulting PSQ-SH was dried in the oven at 60°C for 24 h.

2.1.3. Preparation of CNTs-PSQ. CNTs-PSQ was prepared by the click chemistry according to the following procedures: 0.3 g of PSQ-SH was dissolved in 5 mL of PDA-coated CNT

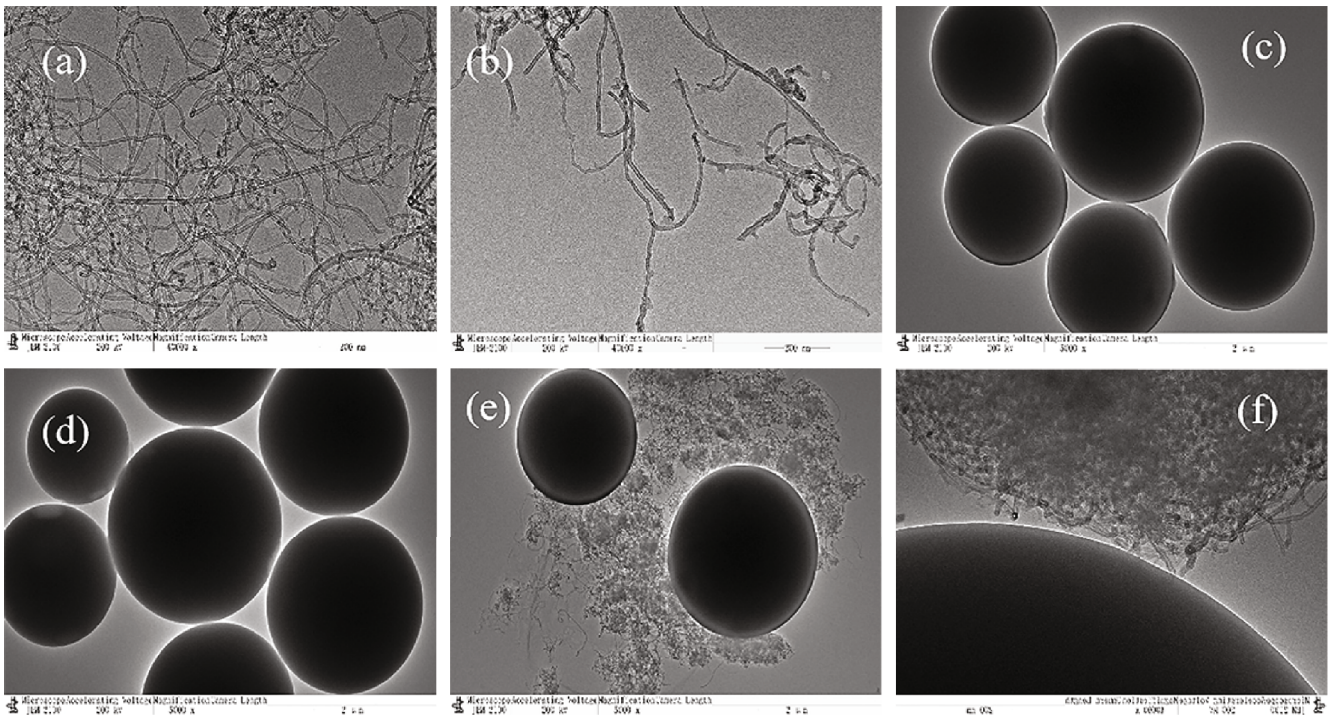

Figure 4: (a) TEM images of raw CNTs. (b) TEM images of CNTs-PDA. (c, d) TEM images of PSQ-SH particle. (e, f) TEM images of CNTs-PSQ.

solution (26 mg mL^{-1} in THF solvent), followed by the addition of 5 mg of DMPA, and reacted for 30 min under ultraviolet light. The resultant products were filtered using a microporous membrane, washed repeatedly with ethanol and deionized water, and dried in an oven at 60°C for 24 h.

The whole synthesis route of CNTs-PSQ is shown in Figure 1.

2.2. Characterization

2.2.1. Fourier Transform Infrared (FTIR) Spectroscopy. FTIR spectra were recorded on a Nicolet FTIR-Magna-750 spectrophotometer (Thermo Nicolet Corporation, Madison, WI, USA) in the range of 4000-400 cm^{-1} by total reflection mode.

2.2.2. X-Ray Diffraction (XRD). XRD patterns were carried out using a Rigaku D/max RB X-ray diffractometer (Tokyo, Japan) with diffraction angles from 5° to 60°. CuKα ($\lambda = 0.154$ nm) was used as the X-ray source with a generator voltage of 40 kV and a current of 100 mA.

2.2.3. Thermogravimetric Analysis (TGA). The TGA analysis was conducted using a NETZSCH Group 209F1 thermogravimetric analysis instrument (Germany) ranging from 20°C to 800°C at a heating rate of 10°C min^{-1} under N_2 protection.

2.2.4. Scanning Electron Microscopy (SEM). SEM analysis was performed on a JMS-6700F (JEOL, Mitaka, Japan) scanning microscope equipped with an energy-dispersive X-ray (EDX ISIS 300, Oxford, UK) microanalytical system. The samples were cryofractured in liquid nitrogen prior to SEM testing.

2.2.5. Transmission Electron Microscopy (TEM). For the transmission electron microscopy (TEM) analysis, the specimens were cut into pieces of ~100 nm in thickness through an ultrathin section using UC7-532319 (Leica, Solms, Germany) microtome under a liquid nitrogen atmosphere. Then, the observations were carried out on a JEM-3010 (UHR, JEOL, Japan) transmission electron microscope at an acceleration voltage of 100 kV.

2.2.6. Thermal Conductivity. The thermal conductivity of the polymer composites was collected from a DTC-300 (TA).

2.2.7. Dielectric Characteristics. Dielectric performance was analyzed using an Alpha-A (Novocontrol Technologies, Montabaur, Germany) Novocontrol at a frequency sweeping from 10^7 to 10^{-2} Hz with a voltage of 1 V at room temperature. The samples were subjected to gold sputtering for 100 s before testing.

3. Results and Discussion

FT-IR analysis can evaluate the complete polyhedral cages, incomplete open cages and random network/short ladder structures of carbon nanotubes, and well-defined siloxane models. As shown in Figure 2(a), the absorption at 2940 cm^{-1} is assigned to the characteristic absorption peak of methylene. The peak at 1089 cm^{-1} is attributed to the characteristic absorption peak of Si-O-Si on carboxylic acid, which is divided into two absorption peaks after the hydrolysis polymerization reaction. Generally, the frequency at 1030 cm^{-1} which arises from the Si-O-Si stretch symmetric vibration from the inversion point of the $(Si\text{-}O)_n$ ring is

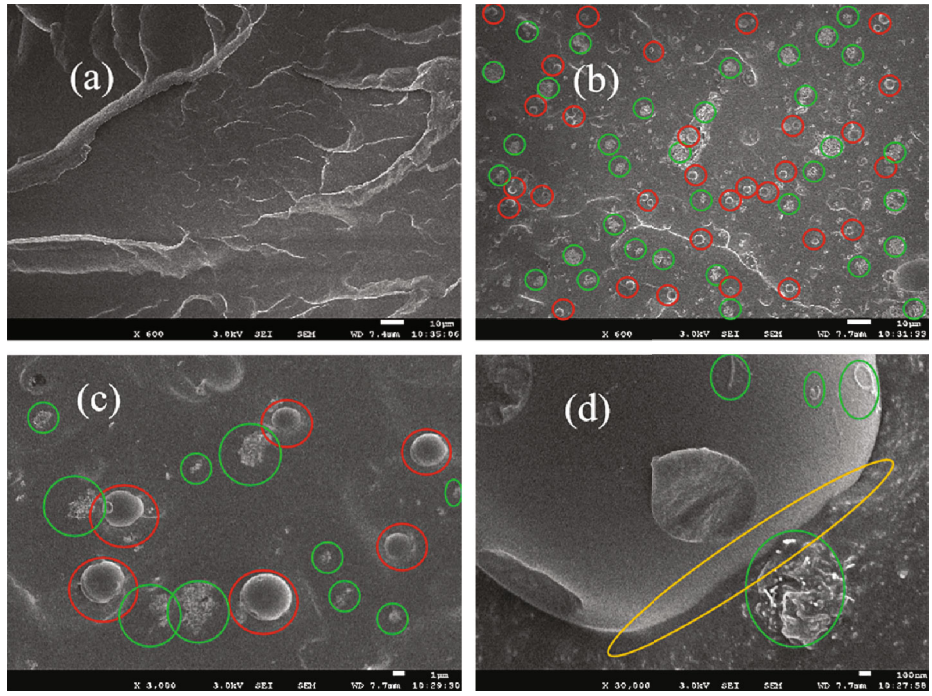

FIGURE 5: (a) SEM images of silicon rubber. (b, c) SEM images of silicon rubber-based nanocomposites with CNTs-PSQ. (d) SEM images of interface between CNTs, PSQ, and SR matrix.

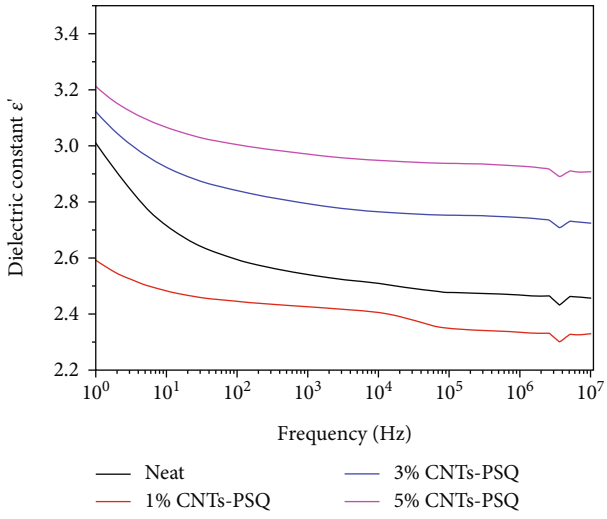

FIGURE 6: Dielectric constant ε' versus frequency for the nanocomposites with various addition of CNTs-PSQ.

sensitive to the microstructure, as its intensity is large for low symmetry silsesquioxane structures such as branched random networks. And the intensity of the frequency at around 1125 cm^{-1}, which arises from multiple Si-O-Si asymmetric stretching vibrations, is intensive due to the existence of $(Si\text{-}O)_4$ ring. It can be seen from Figure 2(b) that the broadband closed to 3443 cm^{-1} is attributed to the amine group stretching vibration, and the absorption peak at 1251 cm^{-1} is ascribed to the hydroxyl stretching vibrations of benzene. These results collectively demonstrate the successful surface modification of CNTs by PDA. Furthermore, two intensive absorption peaks at 2930 cm^{-1} and 2853 cm^{-1} are attributed to the stretching vibration band of methylene, respectively. And the characteristic peaks at 1030 cm^{-1} and 1125 cm^{-1} are ascribed to the Si-O-Si vibration of PSQ, which illustrate the successful fabrication of CNTs-PSQ.

Raman spectroscopy is utilized to detect the functional CNTs with the D band and G band, which corresponded to the peaks at 1353 cm^{-1} and 1593 cm^{-1}, respectively. The I_D/I_G intensity ratio is generally used to appraise the microstructural quality of CNTs. From Figure 2(c), compared with CNTs, the I_D/I_G of CNTs-PDA and CNTs-PSQ changed from 0.89 to 0.38, indicating the compensation of some defects on the CNT surface with negligible change in the structures of CNTs. The above-mentioned evidences have clearly demonstrated that the PSQ-SH is successfully grafted on CNT surface by mussel-inspired chemistry and click chemistry.

The powder XRD technique is widely used for the structure analysis of ladder polymers. In this paper, XRD analysis is carried out to investigate the CNTs and PSQ-SH structures in detail. As shown in Figure 2(d), the ladder-like polysilsesquioxane typically shows two characteristic diffraction peaks which appeared at $2\theta = 7.5^\circ$ and $2\theta = 21.4^\circ$. According to the literature review [30], the peaks at $2\theta = 7.5^\circ$ and $2\theta = 21.4^\circ$ are attributed to the ladder width and thickness of the ladder superstructure, respectively, while CNTs possess two diffraction peaks at the positions of $2\theta = 26.2^\circ$ and 44.3°, corresponding to the (002) and (101) crystal faces of carbon materials, respectively. The product CNTs-PSQ still maintains their original structure of the introduction of CNTs and PSQ.

TGA analysis is adopted to investigate the thermal stability of the CNTs and PSQ-SH. As shown in Figures 2(e)

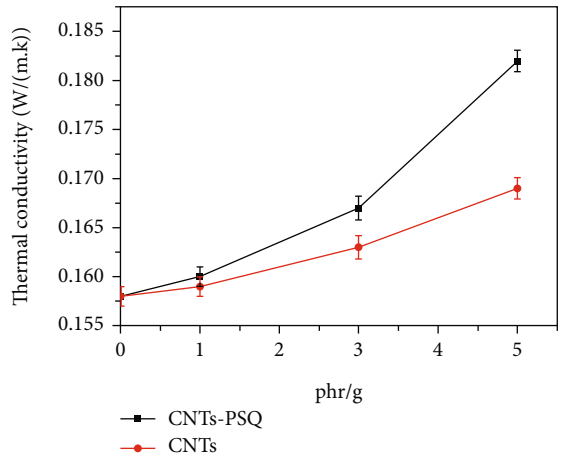

Figure 7: Thermal conductivity versus CNTs-PSQ and CNTs nanoparticle content for the nanocomposites.

and 2(f), the TGA curves of KH590 and PSQ-SH behave completely different. Compared with KH590, the thermal stability of PSQ-SH is greatly improved due to its unique cage structure. The initial thermal decomposition temperature of PSQ-SH exceeds 350°C, and the cage structure remains relatively stable even at 800°C. At the same time, carbon nanotube is a kind of material with excellent thermal stability. There is no weight loss of pristine CNTs when the temperature is up to 800°C. After modification with PDA, with the increase of temperature, it is obvious that CNTs-PDA gradually decomposes gently and uniformly. Due to the superposition of polydopamine and PSQ, the thermal degradation of CNTs-PSQ is further exacerbated. Although the thermal stability of the modified CNTs decreases, it could still sustain good thermal stability at 300°C.

To in-depth verify the surface modification of CNTs, SEM is conducted to detect the change of morphology of CNTs, CNTs-PDA, and CNTs-PSQ. Compared with Figures 3(a) and 3(b), it could be seen that the carbon nanotubes coated with dopamine become coarser with a certain disorder. And Figure 3(c) shows the micromorphology of PSQ-SH particles. The micromorphology of PSQ-SH displays an obvious spherical structure with the approximate diameter of 3-5 μm. At the same time, the cross-section image from Figure 3(d) indicates that the microstructure is a solid sphere. In Figure 3(e), it can be viewed that a good dispersion effect between the dopamine-coated CNTs and PSQ microspheres is realized, which means that the PSQ microspheres can be uniformly coated with carbon nanotubes. From the enlarged SEM image of Figure 3(f), there is a strong interface interaction between carbon nanotubes and PSQ microspheres, and a small number of carbon nanotubes are attached to the surface of PSQ microspheres.

Figure 4 depicts the TEM photographs of CNTs, CNTs-PDA, and CNTs-PSQ. As presented in Figures 4(a) and 4(b), carbon nanotubes are easily entangled inorganic nanosized fillers. The microscopic morphology of spherical PSQ is shown in Figures 4(c) and 4(d), and the particle size of PSQ-SH was about 3-5 μm, while PSQ also tends to aggregate together before modification. Figures 4(e) and 4(f) show that the wrapping of carbon nanotubes can facilitate the better dispersion of PSQ, and there is a strong interface interaction between CNTs and PSQ. Considering the SEM and TEM morphologies, we can conclude that the CNTs and PSQ have good interface effects and dispersion morphology, which provides a guarantee for achieving good dispersion in rubber.

The surface morphology of the silicon rubber-based nanocomposites incorporated with CNTs-PSQ is demonstrated in Figure 5. The comparison between Figures 5(a) and 5(b) shows that CNTs (green ring) and PSQ (red ring) are evenly dispersed in the silicon rubber matrix. And it is clearly seen in Figure 5(c) that both the CNTs and PSQ could form strong interfacial interaction with the rubber matrix. Figure 5(d) shows that there existed obvious interfacial interaction between the silicon rubber, CNTs, and PSQ. The uniform dispersion of nanoparticles and the good interface between nanoparticles and matrix materials are beneficial for increasing the thermal conductivity of the polymer matrix.

The dielectric constant (ε') as a function of frequency for these nanocomposites is displayed in Figure 6. The ε' value increases firstly and then decreases with the increase of filler contents. However, the change range of the dielectric constant is extremely small, which is considered as the insulating rubber. In other words, after the addition of nanofillers, the SR/CNTs-PSQ composites could still demonstrate excellent insulating characteristics.

Figure 7 displays the thermal conductivity of the silicon rubber-based nanocomposites. It is universally acknowledged that the high thermal conductivity could enhance the service life of the rubber-based composites by facilitating heat transfer. As we all know, CNTs have excellent thermal conductivity (2000-3000 $W\,m^{-1}\,K^{-1}$). Therefore, as expected, the inclusion of CNTs and PSQ could significantly improve the thermal conductivity of the silicon rubber-based nanocomposites, which is consistent with the reported literature [4–6]. However, when CNTs are used alone, the improvement of the thermal conductivity is severely limited due to the poor dispersion and interfacial interaction of carbon nanotubes in the rubber matrix. Furthermore, the thermal conductivity of SR nanocomposites increases steadily by increasing the concentration of CNTs-PSQ up to 5 phr. The incorporation of 5 phr CNTs-PSQ into the silicon rubber matrix enhance the thermal conductivity of specimens by 15.2%.

4. Conclusion

In this work, inspired by the mussel bionic technology and click chemistry, CNTs-PSQ nanoparticles were fabricated by chemical bonding between carbon nanotubes and polysilsesquioxane, which effectively solved the problems of easy agglomeration of carbon nanotubes and poor interface bonding with rubber matrix. The micromorphology and chemical structures of CNTs-PSQ were determined by combining FT-IR, Raman, XRD, TGA, SEM, and TEM analyses.

The PSQ coatings could not only significantly enhance the dispersion uniformity of CNTs into the SR matrix but also form stronger interfacial interaction between CNT nanoparticles and SR matrix. Therefore, the SR/CNTs-PSQ nanocomposites exhibited simultaneously improved thermal conductivity and insulation performance, which provides a novel strategy for the preparation of well-distributed CNTs and high-performance rubber materials for electronic components.

Data Availability

Some or all data, models, or code generated or used during the study are available in a repository or online in accordance with funder data retention policies (provide full citations that include URLs or DOIs).

Conflicts of Interest

The authors declare that they have no known competing financial interests or personal relationships that could have appeared to influence the work reported in this paper.

Acknowledgments

This work was supported by grant from the Natural Science Foundation of Shandong Province (ZR2020ME059 and ZR2021ME028).

References

[1] F. Hu, Z. P. Xie, J. Zhang, Z. L. Hu, and D. An, "Promising high-thermal-conductivity substrate material for high-power electronic device: silicon nitride ceramics," *Rare Metals*, vol. 39, no. 5, pp. 463–478, 2020.

[2] S.-W. Xiong, P. Zhang, Y. Xia, Q. Zou, M.-y. Jiang, and J.-G. Gai, "Unique antimicrobial/thermally conductive polymer composites for use in medical electronic devices," *Journal of Applied Polymer Science*, vol. 138, no. 13, p. 50113, 2021.

[3] A. Siricharoenpanich, S. Wiriyasart, A. Srichat, and P. Naphon, "Thermal cooling system with Ag/Fe_3O_4 nanofluids mixture as coolant for electronic devices cooling," *Case Studies in Thermal Engineering*, vol. 20, article 100641, 2020.

[4] Y. Y. Gao, M. H. Zhang, X. R. Chen et al., "A high-performance thermal conductive and outstanding electrical insulating composite based on robust neuron-like microstructure," *Chemical Engineering Journal*, vol. 426, article 131280, 2021.

[5] H. Y. Guo, T. L. Xu, S. S. Zhou et al., "A technique engineered for improving thermal conductive properties of polyamide-6 composites via hydroxylated boron nitride masterbatch-based melt blending," *Composites Part B: Engineering*, vol. 212, article 108716, 2021.

[6] S. G. Li, X. M. Hou, S. X. Lu et al., "Fabrication and simulation of a layered ultrahigh thermal conductive material made of self-assembled graphene and polydopamine on a copper substrate," *RSC Advances*, vol. 11, no. 55, pp. 34676–34687, 2021.

[7] Y. Yusof, M. I. Zaidi, and M. R. Johan, "Enhanced structural, thermal, and electrical properties of multiwalled carbon nanotubes hybridized with silver nanoparticles," *Journal of Nanomaterials*, vol. 2016, Article ID 6141496, 9 pages, 2016.

[8] V. Kumar and D. J. Lee, "Studies of nanocomposites based on carbon nanomaterials and RTV silicone rubber," *Journal of Applied Polymer Science*, vol. 134, no. 4, 2017.

[9] E. Natarajan, C. S. Hassan, A. Chun Kit, M. S. Santhosh, S. Ramesh, and R. Sasikumar, "Modeling of multiwall carbon nanotubes reinforced natural rubber for soft robotic applications - a comprehensive presentation," *Materials Today: Proceedings.*, vol. 46, pp. 3251–3258, 2021.

[10] S. Wang, Y. F. Huang, E. S. Chang et al., "Evaluation and modeling of electrical conductivity in conductive polymer nanocomposite foams with multiwalled carbon nanotube networks," *Chemical Engineering Journal*, vol. 411, article 128382, 2021.

[11] L. S. Salah, N. Ouslimani, M. Chouai, Y. Danlee, I. Huynen, and H. Aksas, "Predictive optimization of electrical conductivity of polycarbonate composites at different concentrations of carbon nanotubes: a valorization of conductive nanocomposite theoretical models," *Materials*, vol. 14, no. 7, 2021.

[12] A. Vozniakovskii, A. Voznyakovskii, S. Kidalov, E. Ovchinnikov, and E. Kalashnikova, "Thermal conductivity and heat capacity of nanofluid based on water modified by hybrid material of composition detonation nanodiamonds-carbon nanotubes," *Fullerenes, Nanotubes and Carbon Nanostructures*, vol. 30, no. 1, pp. 5–9, 2022.

[13] M. Desa, A. Hassan, A. Arsad, R. Arjmandi, and N. N. B. Mohammad, "Influence of rubber content on mechanical, thermal, and morphological behavior of natural rubber toughened poly(lactic acid)-multiwalled carbon nanotube nanocomposites," *Journal of Applied Polymer Science*, vol. 133, no. 48, 2016.

[14] E. Harea, R. Stocek, L. Storozhuk, Y. Sementsov, and N. Kartel, "Study of tribological properties of natural rubber containing carbon nanotubes and carbon black as hybrid fillers," *Applied Nanoscience*, vol. 9, no. 5, pp. 899–906, 2019.

[15] F. Afsharirad, S. Mousanezhad, H. Biglari, and O. Rahmani, "Molecular dynamics of axial interwall van der Waals force and mechanical vibration of double-walled carbon nanotubes," *Materials Today Communications*, vol. 28, 2021.

[16] P. H. Ying, J. Zhang, Y. Du, and Z. Zhong, "Effects of coating layers on the thermal transport in carbon nanotubes-based van der Waals heterostructures," *Carbon*, vol. 176, pp. 446–457, 2021.

[17] Y. X. Liang, H. Y. Zhai, B. Y. Liu, M. Ji, and J. Li, "Carbon nanomaterial-modified graphite felt as an anode enhanced the power production and polycyclic aromatic hydrocarbon removal in sediment microbial fuel cells," *Science of The Total Environment*, vol. 713, no. 9, article 136483, 2020.

[18] Z. Li, K. Otsuka, D. Yamashita, D. Kozawa, and Y. K. Kato, "Quantum emission assisted by energy landscape modification in pentacene-decorated carbon nanotubes," *ACS Photonics*, vol. 8, no. 8, pp. 2367–2374, 2021.

[19] L. Baharudin, A. C. K. Yip, V. B. Golovko, M. I. J. Polson, K. F. Aguey-Zinsou, and M. J. Watson, "CO oxidation and the inhibition effects of carboxyl-modification and copper clusters on multi-walled carbon nanotubes," *Applied Catalysis B: Environmental*, vol. 262, no. 16, article 118265, 2020.

[20] Y. Zhang, J. Liu, Z. Fang, X. Lin, W. Zhang, and D. Yu, "Polyaniline/pure carbon assemblies as efficient self-standing metal-free oxygen electrodes in alkaline media for Zn-air batteries," *Chemistry – An Asian Journal.*, vol. 15, no. 10, pp. 1544–1548, 2020.

[21] M. Bilal, T. A. Nguyen, and H. M. N. Iqbal, "Multifunctional carbon nanotubes and their derived nano-constructs for enzyme immobilization - a paradigm shift in biocatalyst design. Review," *Coordination Chemistry Reviews*, vol. 422, article 213475, 2020.

[22] S. C. Chen, K. T. Chen, and A. F. J. Jou, "Polydopamine-gold composite-based electrochemical biosensor using dual-amplification strategy for detecting pancreatic cancer-associated microRNA," *Biosensors and Bioelectronics*, vol. 173, article 112815, 2021.

[23] S. M. Kang, S. Park, D. Kim, S. Y. Park, R. S. Ruoff, and H. Lee, "Simultaneous reduction and surface functionalization of graphene oxide by mussel-inspired chemistry," *Advanced Functional Materials*, vol. 21, no. 1, pp. 108–112, 2011.

[24] W. G. Wang, J. K. Sun, Y. Q. Zhang et al., "Mussel-inspired tannic acid/polyethyleneimine assembling positively-charged membranes with excellent cation permselectivity," *Science of The Total Environment*, vol. 817, article 153051, 2022.

[25] Y. Q. Zhang, J. Guo, G. Han et al., "Molecularly soldered covalent organic frameworks for ultrafast precision sieving," *Science Advances*, vol. 7, no. 13, article eabe8706, 2021.

[26] H. Lee, S. M. Dellatore, W. M. Miller, and P. B. Messersmith, "Mussel-inspired surface chemistry for multifunctional coatings," *Science*, vol. 318, no. 5849, pp. 426–430, 2007.

[27] W. Wang, Y. Zhang, F. Li et al., "Mussel-inspired polyphenol/polyethyleneimine assembled membranes with highly positive charged surface for unprecedented high cation perm-selectivity," *Journal of Membrane Science*, vol. 658, article 120703, 2022.

[28] M. Saeed, S. Beigi-Boroujeni, S. Rajabi, G. R. Ashteiani, M. Dolatfarahi, and M. Ozcan, "A simple, green chemistry technology for fabrication of tissue-engineered scaffolds based on mussel-inspired 3D centrifugal spun," *Materials Science and Engineering: C*, vol. 121, article 111849, 2021.

[29] W. J. Li, H. Liu, Y. Y. Mi et al., "Robust and conductive hydrogel based on mussel adhesive chemistry for remote monitoring of body signals," *Friction*, vol. 10, no. 1, pp. 80–93, 2022.

[30] M. Liang, C. P. He, J. D. Dai et al., "A high-strength double network polydopamine nanocomposite hydrogel for adhesion under seawater," *Journal of Materials Chemistry B*, vol. 8, no. 36, pp. 8232–8241, 2020.

[31] Y. J. Chen, Q. Q. Wang, D. W. Li et al., "Mussel-inspired double cross-linked hydrogels with desirable mechanical properties, strong tissue-adhesiveness, self-healing properties and antibacterial properties," *Materials Science and Engineering: C*, vol. 120, article 111690, 2021.

[32] S. N. Zhou, H. X. Ji, L. J. Liu et al., "Mussel-inspired coordination functional polymer brushes-decorated rGO-stabilized silver nanoparticles composite for antibacterial application," *Polymer Chemistry*, vol. 11, no. 16, pp. 2822–2830, 2020.

[33] Z. X. Zhang, J. K. Hao, P. Xie, X. J. Zhang, C. C. Han, and R. B. Zhang, "A well-defined ladder polyphenylsilsesquioxane (Ph-LPSQ) synthesized via a new three-step approach: monomer self-organization-lyophilization-surface-confined polycondensation," *Chemistry of Materials*, vol. 20, no. 4, pp. 1322–1330, 2008.

[34] M. N. Temnikov, V. G. Vasil'ev, M. I. Buzin, and A. M. Muzafarov, "Synthesis and comparison of the rheological and thermal properties of acyclic and polycyclic forms of polyphenylsilsesquioxane," *European Polymer Journal*, vol. 130, article 109676, 2020.

[35] H. J. Hao, X. Y. Zhou, Z. H. Shen, J. Y. He, and R. J. Yang, "Study on the ablative properties of ethylene propylene diene terpolymer/silsesquioxane insulation materials," *Journal of Applied Polymer Science*, vol. 137, no. 6, article 48365, 2020.